Calculational Approach and Results of the Safe Shutdown Earthquake Event for the Pebble Bed Modular Reactor

Gert van Heerden, Sonat Sen, Frederik Reitsma*
Reactor Design and Fuel Management Group, PBMR Pty Ltd,
PO Box 9396, Centurion, 0046, South Africa.

Abstract

The Pebble Bed Modular Reactor (PBMR) concept can be described as a high-temperature helium-cooled, graphite-moderated pebble-bed reactor with a multi-pass fuelling scheme. The fuel is contained in 6 cm diameter graphite spheres containing carbon-based coated UO_2 kernels. An online fuel reload scheme is applied with the fuel spheres being circulated through the reactor. The pebble-bed reactor core thus consists of fuel pebbles packed in the core cavity in a random way.

The packing densities and pebble flow is well known through analysis and tests done in the German experimental and development program. The pebble-bed typically has a packing fraction of 0.61. In the event of an earthquake this packing fraction may increase with the effect that the core geometry and core reactivity will change.

The Safe Shutdown Earthquake (SSE) analysis performed for the PBMR 400 MW design is described in this paper, and it specifically covers SSE-induced pebble-bed packing fractions of 0.62 and 0.64. The main effects governing the addition of reactivity in the SSE event are the changes in core neutronic leakage due to the decreased core size and the decreased effectiveness of the control rods as the pebble-bed height decreases. This paper describes the models, methods and tools used to analyse the event, the results obtained for the different approaches and the consequences and safety implications of such an event.

KEYWORDS: PBMR, packing fraction, safe shutdown earthquake, transients, Tinte

1. Introduction

The Pebble Bed Modular Reactor (PBMR) concept can be described as a high-temperature helium-cooled, graphite-moderated pebble-bed reactor with a multi-pass fuelling scheme. A detailed description of the plant design, specifically the reactor core neutronics design, has been published [1,2,3]. In pebble-bed reactors the fuel is embedded in 6 cm diameter graphite spheres containing carbon-based triso-coated UO_2 kernels. In the PBMR annular core the fuel spheres are packed in a random way and the typically achieved average packing fraction (1 – void fraction) is assumed to be 0.61. It is important to understand the behaviour of a pebble-bed under normal

* Corresponding author, Tel. +27-12 677 9934, Fax +27-12 663 8797, E-mail: frederik.reitsma@pbmr.co.za

operation (see reference [4] for example) but the focus of the work presented here is on the effects that a postulated change in the bulk or average packing density during an earthquake will have on the core-neutronics and thermal-hydraulics behaviour of the PBMR.

The variation in the packing fraction in pebble-beds during earthquakes has been studied in detail in the SAMSON [5] shaker-table experiments, located at the HRG (Hochtemperatur-Reaktorbau GmbH) site at Jülich, Germany. This was used to postulate conservative compaction densities and times for use in the safety studies presented here. This is described in Section 2 with the models and calculational approach detailed in Section 3. The results and a discussion of the phenomena observed are included in Section 4, followed by the conclusions.

2. The Postulated Safe Shutdown Earthquake

The effect of the postulated Safe Shutdown Earthquake (SSE) event on the Reactor Unit (RU) is translated into a compaction of the pebble-bed or fuel region only. No radial disturbance in the core cavity dimensions are modeled since these are excluded by the core structure and graphite reflector design. Therefore, the only effect of the pebble-bed compaction is a decrease in the pebble-bed height. The change in pebble-bed height is accompanied by a reactivity insertion due to the denser packing of the fuel spheres as well as a simultaneous reduction in the control rod effectiveness (the insertion depth is reduced relative to the top of the pebble-bed).

It is assumed that during a given SSE the packing fraction of the fuel pebbles increases from the nominal 0.61 to a higher value. This paper reports on two pebble-bed compaction cases, namely, an increase in packing fraction to 0.62 and also to 0.64. The 0.62 represents a realistic but conservative estimate for the PBMR reactor, whereas the 0.64, being the upper limit for randomly packed spheres, represents an extreme and bounding case for a pebble-bed core [6]. Also, each of the compaction cases was analysed for compaction durations of 5 seconds and 15 seconds respectively, which represent the typical range for the duration of strong shaking that results from large earthquakes.

In addition to the compaction effects it is postulated that the SSE includes a loss of coolant circulation; a PLOFC (Pressurised Loss of Forced Cooling) is defined as the design basis accident and a DLOFC (Depressurised Loss of Forced Cooling) as the beyond-design-basis accident.

The chosen packing fraction of 0.64 for the SSE event is very conservative and such a high packing fraction would be the end result of shaking a pebble-bed for a very long time (compared to the typical earthquake duration). Thus, the cases which assume that the maximum packing fraction (0.64) could be attained in 5 seconds or 15 seconds, are in fact hypothetical. Although those cases are not realistic, they still provide valuable insights with respect to limiting or bounding values for the neutronic and thermal response of a pebble-bed reactor. The SAMSON shaker-table experiments indicated a much smaller pebble solid faction increase; from 0.61 to 0.613 for a 5 second duration, and an increase to 0.616 for a 15 second duration, both attained at a 0.4g peak acceleration [7]. The change in core packing ratio will cause a reduction of about 0.177 m and 0.516 m in the total pebble-bed height, and with the same increase in the height of the cavity above the core, for the 0.62 and 0.64 compaction fractions respectively.

In the event of an earthquake it is important to quantify the changes in the core reactivity, the fission power and material temperatures, especially the fuel heat-up rate during the power excursion.

3. The Calculational Path and Model Approach

The VSOP99/3 [8] and Tinte [9] codes, developed at the Research Centre Jülich (FZJ) and licensed to PBMR (Pty) Ltd, were used to evaluate the SSE event. In the models the effects of a pebble-bed compaction and reactivity insertion due to the reduced control rod insertion depth (both functions of time) need to be modeled in a manner that corresponds as closely as possible to reality. It is not possible to model all aspects of the SSE event as true functions of time with the available tools. Some simplifications and assumptions were made to provide the best approximate analysis of the event.

The two major phenomena that need to be captured are first the neutronic response of the fuel due to the bed compaction including the subsequent feedback effects, and second, the changes in the heat transfer from the pebble fuel to the adjacent graphite core structures during the loss of cooling events. Since it is not possible to model the pebble-bed geometrical compaction dynamically with Tinte (and very few neutronics codes, if any, do have such capabilities), it therefore necessitates a two-fold approach. An un-compacted Tinte model is used to obtain the conditions just before the SSE event, and a compacted model is used to reflect the end state directly after the SSE event. Consequently, this dual approach implies that the SSE cases were performed with both the Tinte compacted models and the normal operation un-compacted model.

3.1 Geometrical Models

VSOP99 input data was generated for the two compaction cases and also for the two associated control rod insertion depths. First, a case is defined where the pebble-bed is compacted and accompanied by a reduction in the control rod effective insertion depth due to the bed compaction (the actual situation). In the second configuration, only a pebble-bed compaction is simulated by allowing the control rods to follow the pebble-bed compaction so that the insertion depth, relative to the height of the bed, remains the same as before the SSE event. This was done to separate the two effects. The reference and compacted geometrical models are shown in Figure 1, with the axial height in centimeters given on the Y-axis.

The aspects that had to be included in the two VSOP99 models include: i) changes in the geometry, ii) changes in the homogenised number densities due to the higher packing fraction, iii) re-evaluation of spectrum calculations taking the new cell leakage into account, and iv) positioning the control rods correctly. The isotopic distributions from the VSOP99 models are also used to generate the macroscopic cross-section libraries to be used in the Tinte analysis.

In the time-dependent Tinte analysis either the reference or the already compacted end-state geometrical model was used since it is not possible to change the geometry during the transient calculation. The un-compacted model represents the reactor geometry at the start of the SSE event while the compacted geometry represents the end state after a 5-second or 15-second SSE event. The compacted model represents the correct conditions for the rest of the event (PLOFC or DLOFC), calculated over the next 50 hours. It should thus be a better representation of the thermal processes during the initial heat-up and subsequent cool-down process. Both these geometrical models were tested.

Figure 1: Reference and SSE geometrical models in VSOP.

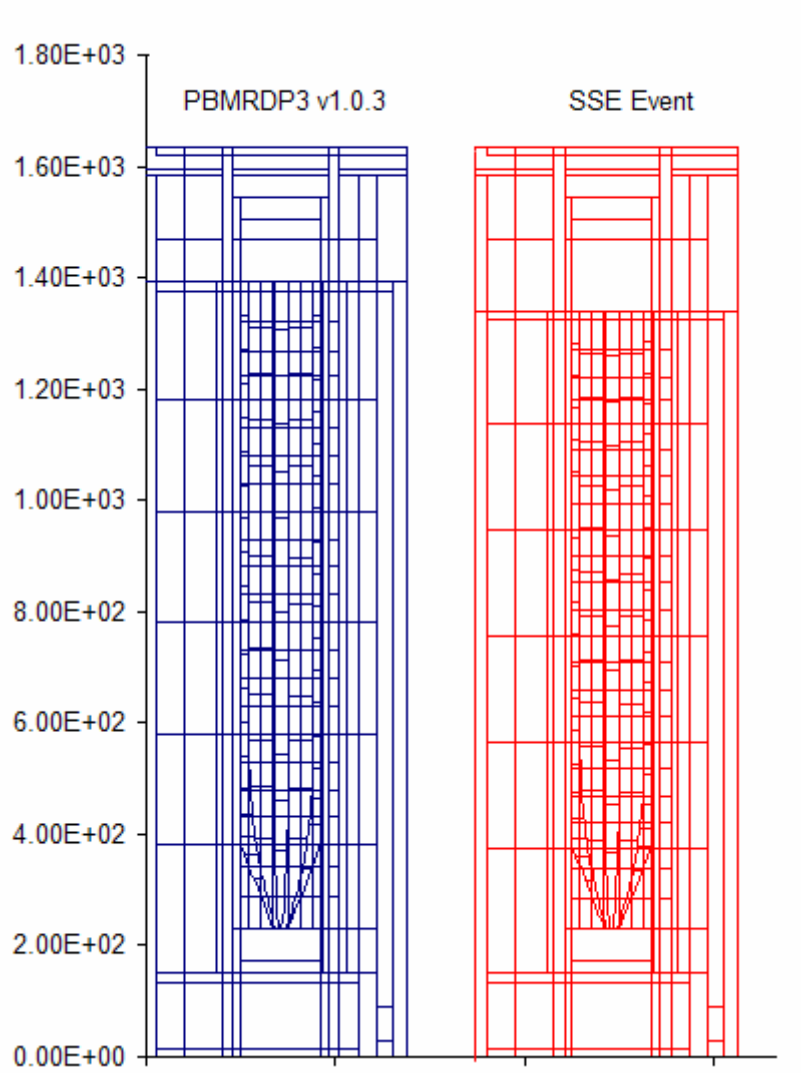

3.2 Case Definitions

The two geometrical models in Tinte were used in the following way. For the reference geometry (un-compacted) the total effect of the SSE reactivity insertion as determined by the VSOP99 analysis was applied as a global reactivity insertion in the pebble bed. We later show that this approach is conservative. Making use of the appropriate compacted model the SSE transient is analysed by introducing the two components of the reactivity insertion separately. The reactivity addition due to the compaction of the pebble-bed is introduced as a global reactivity increase (obtained from the VSOP99 analysis) while the effect of the control rods "being exposed" is simulated as a control rod withdrawal within the Tinte transient. This should capture some of the spatial effects of the control rod's effective removal during the pebble-bed compaction.

The different cases and its associated name are listed in Table 1. The case names will be used

throughout the results section and have the following meaning:

1. TGRI: The un-compacted geometrical model was used for those cases where the total reactivity effect of the core compaction are modeled as a global reactivity insertion (TGRI=Total Global Reactivity Insertion).
2. GRI+CR: The appropriate compacted geometrical models (0.62 or 0.64 packing) were used. The reactivity insertion due to the relative withdrawal of the control rods (CR) are simulated by modeling the rod withdrawal in Tinte whereas only the reactivity increase due to the core leakage effects are modeled as a global reactivity insertion.

In each case the final packing fraction (0.62 or 0.64) and the duration over which the compaction took place (5 sec. or 15 sec.) are also included in the name.

Table 1: SSE cases performed with Tinte

Case name	Geometrical model	CR (Control rods)	Compaction
TGRI_0.62_5s/15s	Un-compacted, CR=202 cm	No movement	0.61 – 0.62 in 5/15 sec.
GRI+CR_0.62_5s/15s	Compacted 0.62, CR=218 cm	Withdrawal, ~218 cm to 202 cm	0.61 – 0.62 in 5/15 sec.
TGRI_0.64_5s/15s	Un-compacted, CR=202 cm	No movement	0.61 – 0.64 in 5/15 sec.
GRI+CR_0.64_5s/15s	Compacted 0.64, CR=248 cm	Withdrawal, ~248 cm to 202 cm	0.61 – 0.64 in 5/15 sec.

The SSE events were calculated as a design basis accident (PLOFC) and a beyond-design-basis accident (DLOFC) associated with the SSE. In all these cases the depressurization and the loss of active cooling were assumed to take place over 5 seconds and directly after the reactivity insertion terminated. In this time the mass flow rate decreased from the normal 192.7 kg/s to zero and the outlet pressure from ~9MPa to 6.0 MPa for the PLOFC and atmospheric pressure for the DLOFC, respectively. All changes during the event were assumed to be linear, including the reactivity insertion.

4. Results

4.1 Steady-state Cases

The reactivity additions during the SSE event were obtained from the steady-state VSOP99 calculations. The results are shown in Table 2 for the different cases (using the same naming convention as explained before). The control-rod position and packing fraction are shown with the resultant k_{eff}. Note that the control rod positions are given relative to the bottom of the top reflector, a reference point that is not moving during the SSE event. The last column shows the reactivity to be applied to the different Tinte cases. In these VSOP calculations all material temperatures were kept unchanged and thus only the leakage and leakage spectrum effects were

taken into account (in the few-group cross-section updates). This approach was selected since the temperature feedback effect (that would decrease the reactivity value) is taken into account in the time-dependent Tinte analysis.

Table 2: VSOP99 results for different packing fraction and CR cases

Case	CR position (cm)	Packing fraction	k_{eff}	Reactivity ρ
Reference	202	0.61	1.0000	-
TGRI_0.62	202	0.62	1.0041	+0.41%
GRI+CR_0.62	218	0.62	1.0024	+0.24%
TGRI_0.64	202	0.64	1.0127	+1.27%
GRI+CR_0.64	248	0.64	1.0074	+0.74%

The Tinte analysis results, as obtained with the three steady-state models (Uncompacted-0.61, Compacted-0.62 and Compacted-0.64), are presented in Table 3. In order to obtain the correct starting conditions for a Tinte model, all transient runs are preceded by a steady-state analysis. For this SSE event analysis it was assumed that the reactor is at full power operation of 400 MW. For the two compacted models, it was ensured that the helium flow paths, temperature and power distribution, and other quantities are similar to the un-compacted model so that the starting conditions of the event are not changed too much. Table 3 reflects the values of some of the major reactor parameters at full power steady state conditions and show that the thermal and gas flow conditions are indeed similar.

Table 3: Tinte SSE models – Steady-state operating conditions

Description	Units	Un-compacted-0.61	Compacted-0.62	Compacted-0.64
Total Power	MW	400.0	400.0	400.0
Relative reactivity	%	-	+0.12%	+0.32%
Control rod position	cm	202	218	248
Maximum fuel temperature	°C	1084.3	1085.5	1085.7
Core average fuel surface temperature	°C	818.8	818.7	817.6
Coolant inlet temperature	°C	500.0	500.0	500.0
Coolant inlet pressure	MPa	9.0	9.0	9.0
Coolant outlet temperature	°C	896.7	896.7	896.7
Coolant outlet pressure	MPa	8.79	8.77	8.73
Coolant mass flow rate	Kg/s	192.7	192.7	192.7

Some of the effects of the compaction can be seen in the Tinte steady state results. For example, the pressure drop increased with the increased packing fraction. The influence on the

steady-state k_{eff} values, shown as a relative reactivity, is also interesting. Even though the control rods were inserted to the same relative insertion depth as during normal operation, an increase in the reactivity as a function of the packing fraction is seen. This effect was also observed in the VSOP99 results. However, in the Tinte cases the temperature feedback effects were included that would explain the considerable lower reactivity effects seen. The differences could also be due to differences in methods and data but comparisons in the reference normal operation models showed good agreement in general.

It is important to note that the steady-state calculation, which is always performed before the transient analyses, is used to obtain a critical starting condition for the transient. The critical condition is then achieved by adjusting the core global reactivity. The different Tinte SSE models will thus all start from a critical condition but different reactivity insertions are applied in the transient. In each transient run performed the reactivity as calculated by VSOP99 (shown in Table 2) was added as a global reactivity. In the GRI+CR cases this is, of course, in addition to the reactivity insertion due to the control rods being withdrawn from its postulated inserted positions (simulating the reduction of the relative control insertion depth). The Tinte transient results are presented in Section 4.2.

4.2 SSE Transients

The results for the SSE transient cases performed with Tinte are presented in Figures 2 – 7. Figure 2 shows that for a given reactivity insertion (ρ or Δk_{eff} input in the Tinte runs) the fission power peak is lower for the 15-second insertion period than for the 5-second insertion period. The total thermal energy (or heat) produced in the fuel, for a given reactivity insertion, should be more or less the same (will have the same end condition), independent of the time over which the reactivity insertion takes place. Therefore, the peak for the 15-second insertion duration must be lower than for the 5 second insertion duration. For the more realistic 0.62 packing fraction case, it is seen that the fission power values as predicted by the two Tinte models, un-compacted vs. compacted, are very close. Therefore, the manner in which the reactivity is applied in the core is not that important for the 0.62 case.

For the higher, and less realistic, 0.64 compaction case the change in the axial height of the core is much more pronounced, so in this case it is important to model the two reactivity insertion components explicitly. Also, for the 0.64 case the much tighter packing of the fissile material, in the compacted model, produces stronger neutronic feedback effects within the fuel-bearing part of the pebbles, resulting in a lower fission power peak than that of the un-compacted model. Nevertheless, after about 30 seconds into the transient, the graphite moderator feedback becomes important and that causes the fission power, of both the 0.62 and 0.64 cases, to approach that of a PLOFC or a DLOFC without any reactivity insertion.

Since the reactivity insertion is applied as a linear function of time, and through the selected ranges for packing fractions (0.61-0.62 and 0.61-0.64) and compaction durations (5 seconds and 15 seconds), it must be noted that the reactivity insertion rate for the 0.62 packing over 5 seconds is very close to that for the 0.64 packing over 15 seconds (0.0041/5 vs. 0.0127/15). Therefore, the fission power curves for those two particular combinations almost coincide over the first 5 seconds. With respect to fission power, the effect of the SSE-induced reactivity insertion disappears by about 300 seconds into the transient.

Figure 2: Fission power for an SSE event and PLOFC conditions

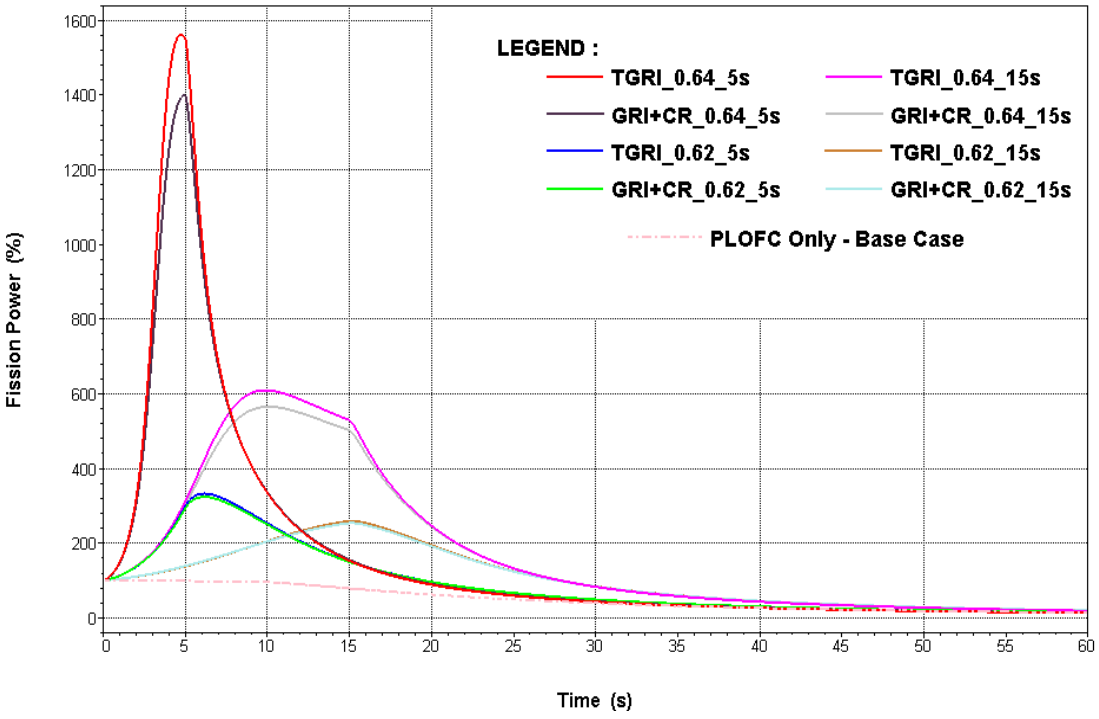

Figure 3: Decay heat for an SSE event and PLOFC conditions

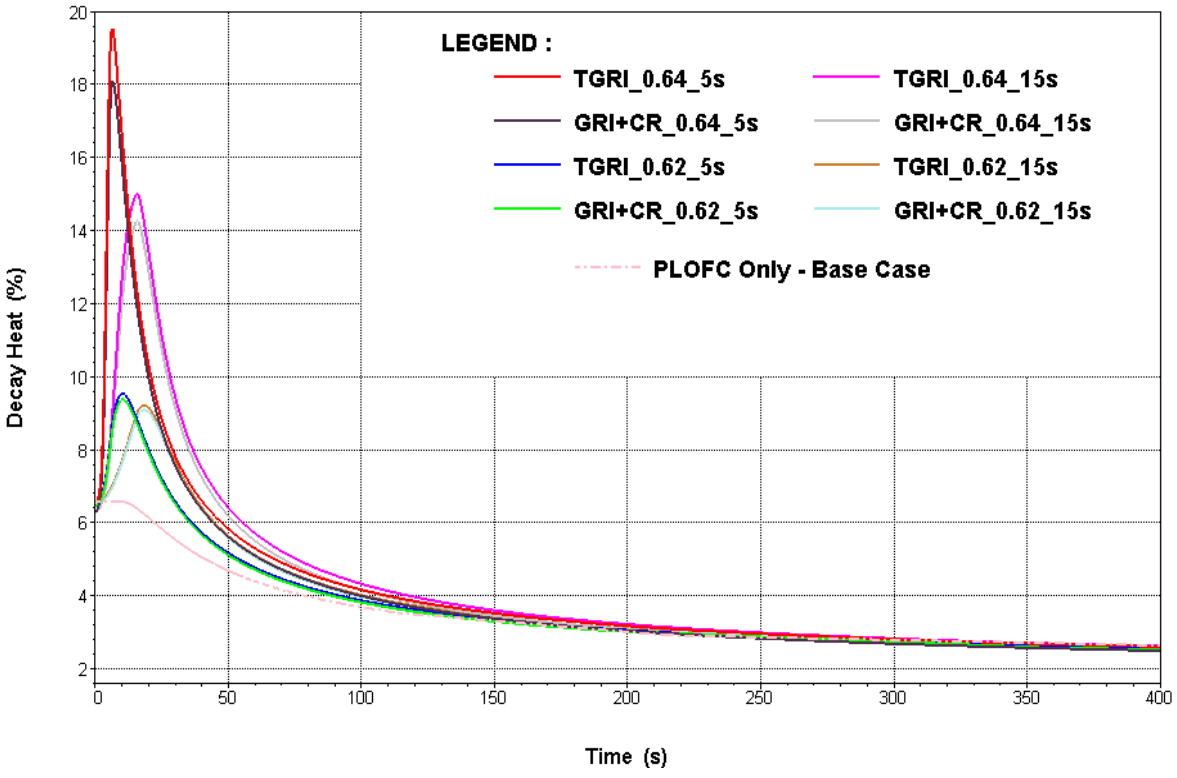

Figure 4: Maximum fuel sphere centre temperatures for an SSE event and PLOFC conditions

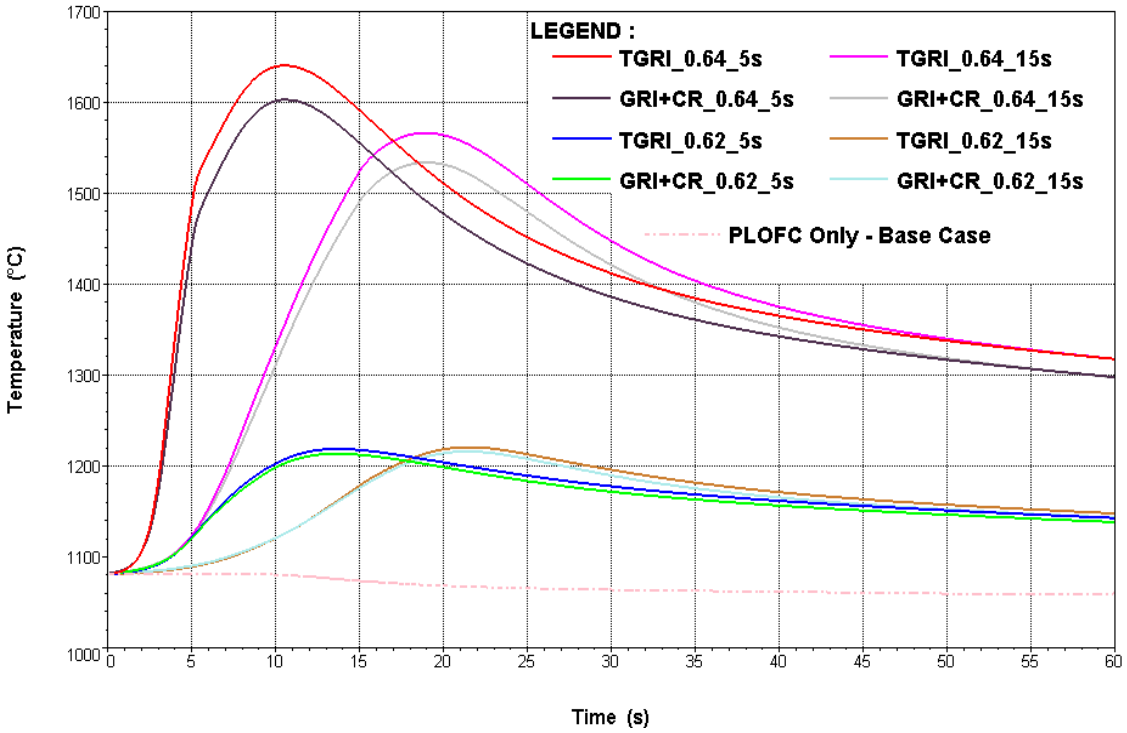

Figure 5: Core average fuel sphere temperatures for an SSE event and PLOFC conditions

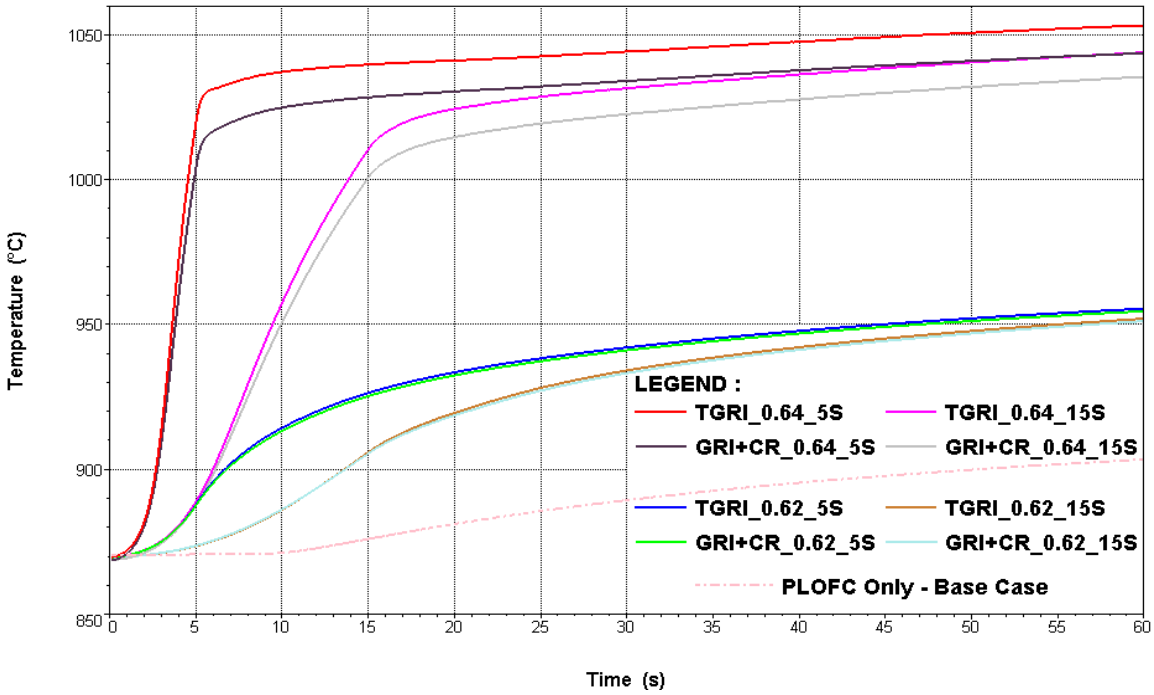

Figure 6: Maximum fuel sphere centre temperature envelopes for an SSE event followed by PLOFC or DLOFC conditions

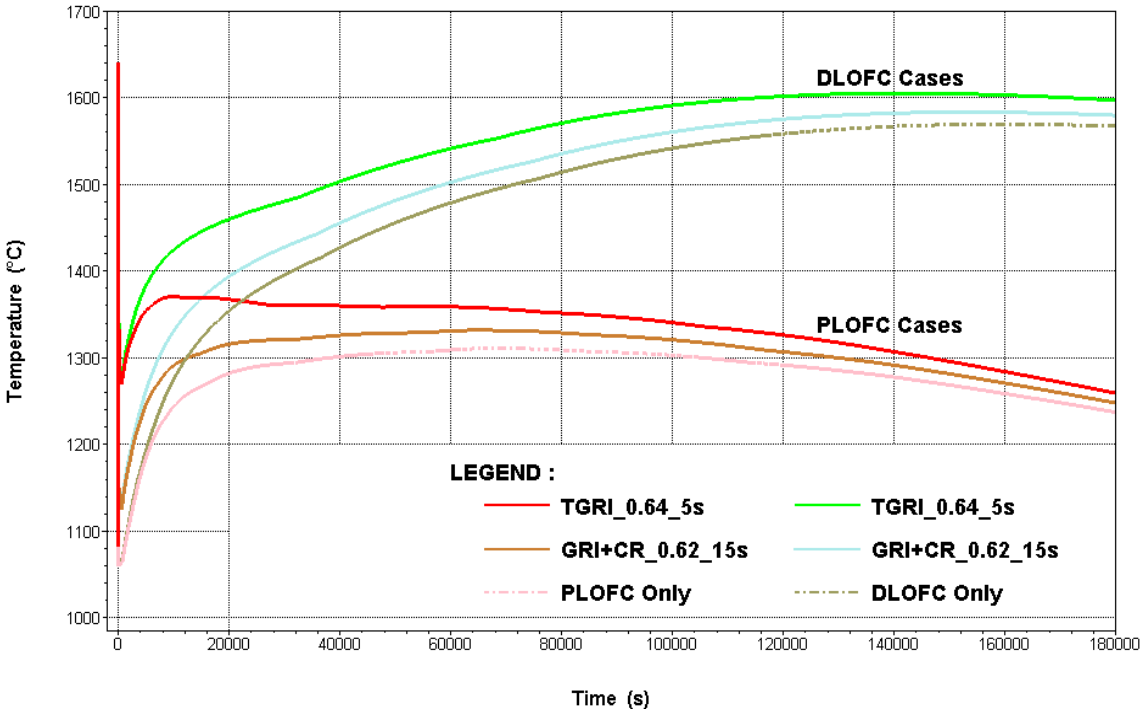

Figure 7: Core average fuel sphere temperature envelopes for an SSE event followed by PLOFC or DLOFC conditions

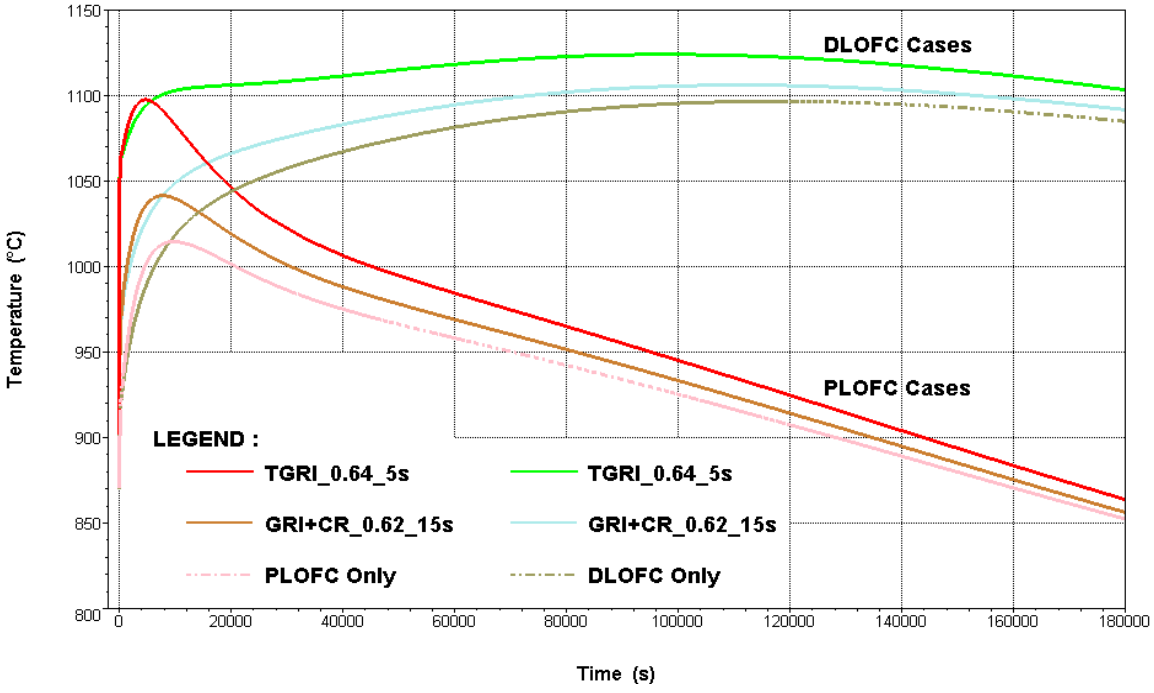

The decay heat curves, expressed as a percentage of the total steady state power (400 MW), is shown in Figure 3. They show behaviour similar to the fission power curves during the period of reactivity insertion. Due to the elevated production of short-lived fission products, the decay heat curves reach their maximum heat output after the reactivity insertion has terminated and the drop down of the decay heat curves becomes purely a function of the decay rate of the short-lived isotopes.

A very important aspect to be aware of is that the Tinte maximum fuel centre temperature represents the maximum value in the core at each time step, and consequently, the position (mesh cell) in which it occurs changes over time. During steady state full power conditions the maximum fuel centre temperature is located towards the lower third of the core. For PLOFC and DLOFC transients the position of maximum fuel centre temperature moves upwards in the core, with some radial outward movement as well, so that it is eventually located in the core where the highest steady state power production occurred. The large heat capacity of the graphite ensures that the temperature rise in the fuel sphere graphite lags behind the rise in fission power. Subsequent to the reactivity insertion, the fission power (or heat production) is determined by the fuel temperature and the rapid decrease in the forced flow over the fuel spheres. These effects are evident in the change in slope of the temperature curves in Figure 4.

The core average fuel temperatures, depicted in Figure 5, also show a rapid rise in temperatures up to the end of the reactivity insertion. Thereafter, the rise in temperatures is determined by the continued heat generation in the fuel spheres (fission and decay heat) as well as the spatial redistribution of the heat energy in the core and also into the adjacent graphite core structures.

Figures 6 and 7 provide the long-term response of a postulated PLOFC or DLOFC subsequent to an SSE event. It is clear, from both figures, that fuel sphere temperatures are dominated by PLOFC conditions early in the event (less than 300 seconds), and by DLOFC conditions over the longer term. The important role that a helium inventory, at 6 MPa, plays in lowering the fuel temperatures is strikingly illustrated on those two figures. In the absence of a helium inventory in the RU, or DLOFC conditions, the low effective thermal conductivity coefficient in the pebble-bed, relative to the other materials in the RU, is responsible for the high fuel temperatures later in the transient. Furthermore, the offset from the base case in both sets of graphs, PLOFC or DLOFC, is an indication of the additional thermal energy generated in the core, resulting from the reactivity insertion as produced by the SSE compaction of the core.

4. Conclusion

A calculational approach to model the SSE event or the PBMR 400MW reactor was developed and implemented making use of the tools available. A Tinte analysis of the neutronic and thermal transient response of the PBMR 400 MW Reactor that follows from a SSE compaction of the fuel spheres in the reactor core requires a dual modeling approach that yields a bounded estimate for the SSE event. Since it is not possible to model the time-dependant compaction of the fuel, an un-compacted model was used to reflect the conditions at the start of the SSE event, and a compacted model was used to represent the conditions at the end of the SSE event. These models were derived from the VSOP99 models.

The main observations, as drawn from the Tinte analysis of the SSE event, are

1. The reactivity insertion produces a rapid upsurge in the fission power with the peak

values reached close to the end of the insertion duration,
2. Strong temperature feedback effects lead to a rapid decline in the fission power and after 300 seconds the fission power is close to the fission power levels that are obtained for a PLOFC without the SSE reactivity insertion,
3. The fuel temperatures also experience a rapid increase, with fuel-centre temperatures reaching a maximum shortly after the SSE induced reactivity insertion has ended,
4. The packing fraction that results from an SSE event has a strong effect on the heat-up rate of the fuel kernels and fuel spheres. The rates that the kernels can sustain without damage to the triso-coated layers are under investigation,
5. For a realistic packing fraction increase, from 0.61 to ~0.62, either of the Tinte models (un-compacted or compacted) could be used to analyse an SSE event,
6. Reactor operating conditions prior to an SSE event, and other than steady state full power, should be investigated to determine which conditions produce the worst impact on fuel heat-up rates and temperatures.

References

1) D. Matzner, "PBMR Project Status and the Way Ahead," Proceedings of 2nd International Topical Meeting on High Temperature Reactor Technology, Beijing, China, 22-24 September, 2004
2) F. Reitsma, "The Pebble Bed Modular Reactor Layout and Neutronics Design of the Equilibrium Cycle," PHYSOR 2004, Chicago, Illinois, April 25-29, 2004, on CD-ROM, American Nuclear Society, Lagrange Park, IL. (2004)
3) IAEA-TECDOC. Draft Title: "Evaluation of High Temperature Gas Cooled Reactor Performance Benchmark analysis related to the PBMR, GT-MHR, HTR-10 and the ASTRA Critical Facility," (In Preparation).
4) C.G. Du Toit, "The Numerical Determination of the Variation in the Porosity of the Pebble-Bed Core," Proc. HTR-TN 2002, April 22-24, Petten, The Netherlands (2002).
5) K.A. Kleine-Tebbe, "SAMSON – A Vibration Test Facility for Simulating Multi-Axis Dynamic Motion," Brown Bovari HRB internal document D HRB 1229 85 E, (1985)
6) F. Kemter, G. Schmidt, "Seismic Behaviour of the Pebble Bed in a HTR Plant," Trans. 8th Int. Conf. SMIRT, Brussels, Belgium, August 19-23, 1985.
7) D. Becker, "Kugelhaufenverdichtung bei Erdbeben", Interatom Internal Report, 38.07204.9 (1988)
8) H. J. Rütten, K. A. Haas, H. Brockmann, U Ohlig, W Scherer "V.S.O.P. (99) for WINDOWS and UNIX computer code system for reactor physics and fuel cycle simulation," Jül –3820
9) H. Gerwin, W. Scherer, and E. Teuchert, 'The TINTE Modular Code System for Computational Simulation of Transient Processes in the Primary Circuit of a Pebble-Bed High-Temperature Gas-Cooled Reactor,' Nucl. Sci. Eng, **103**, 302-312 (1989).